applied sciences

MDPI

Article

Semiempirical Model for Assessing Dewatering Process by Flocculation of Dredged Sludge in an Artificial Reservoir

Bruno Molino [1], Gennaro Bufalo [2], Annamaria De Vincenzo [3] and Luigi Ambrosone [4,*]

1 Department of Bioscience and Territory, University of Molise, 86090 Isernia, Italy
2 INAIL-Sector Research, Certification and Verification, Department of Naples, I-80121 Naples, Italy
3 School of Engineering, University of Basilicata, 85100 Potenza, Italy
4 Department of Medicine and Health Science V. Tiberio, University of Molise, 86100 Campobasso, Italy
* Correspondence: ambroson@unimol.it

Received: 10 March 2020; Accepted: 22 April 2020; Published: 27 April 2020

Abstract: Understanding sedimentation behaviour of clay material is crucial in planning project for sediment removal from bottom of a reservoir. The sedimentation of samples taken from Occhito reservoir (Italy) is investigated. Samples containing and not containing polyacrylamide have been monitored. Results reveal that polymer induces bridging flocculation and the particle-size distribution tends to become uniform. The sedimentation profiles follow a mater curve. Such experimental observation is used to develop a semi-empirical model for assessment of dewatering process by flocculation of dredged sludge in artificial reservoir. A two-step stage model for assessing the volume of solids in a geotextile tube is suggested. Such model is based on the idea that for very long dewatering times solids reach the configuration of free sedimentation.

Keywords: dewatering; sedimentation; flocculant; reservoir; geotextile tube

1. Introduction

A dam blocking a river reduces the natural flow of the solid material causing a continuous decrease in the water capacity of the reservoir [1]. When its actual capacity is less than the initial reservoir storage capacity, the reservoir risks not guaranteeing. the users' demands, thus a planning of *extraordinary management* operations will be necessary [2]. The choice of the site to dispose the dredged material is a crucial point for planning a drainage project [3–5]. Confined disposal was the approach originally employed to treat contaminated material which was neither disposable nor reusable [3]. Therefore, the opportunity to use valid disposal methods for particular classes of dredged material [6,7] must be carefully evaluated through risk analysis [8]. Large diameter geotextile tubes, have been widely used to contain and dehydrate dredged material from river channels and ports [9]. In this approach, coarse-grained sediments, pumped into the geotextile tube, settle quickly and the water is discharged to the outside [10]. In this perspective geotextile tubes assume the role of alternative disposal sites. For instance, sand-filled geotubes are used as artificial banks and peninsulas to stabilize ports or shore protection.

The idea of extending geotextile tubes as dehydration sites for even fine-grained materials has only been analyzed in recent years [11]. If the material to be dehydrated is clayey, the use of geotubes is complicated by the fact that the suspension is made of very fine materials with very long deposition times. To overcome this drawback, polymeric flocculants have been used to accelerate the precipitation of the material in the geotube. It is, therefore, clear that in the dehydration process of clays by means of geotubes, sedimentation plays a key role in planning a dredging project.

The objective of this study is to assess the sedimentation role in the dewatering process, by geotexile tubes, of clayey material dredged from the Occhito reservoir (Italy). Results of sedimentation measurements are used to derive a semi-empirical method to optimize the filling process of geotexile tubes. The sedimentation behavior of mixed and non-mixed with polymers samples allows us to monitor the efficiency of the flocculant in the dewatering process.

2. Materials and Methods

2.1. Materials

Chemical analyzes on samples from Occhito reservoir confirm that the sediment can be labeled as non-hazardous waste. The material is a clay with low values of Al_2O_3 and high CaO content. Samples showed a mineralogical composition mainly characterized by anorthite, ($CaO{\cdot}Al_2O_3$), hillebrandite ($2CaO{\cdot}SiO_2{\cdot}H_2O$), kaolinite ($Al_2O_3{\cdot}2SiO_2{\cdot}2H_2O$), paragonite ($NaAl_2[Si_3Al]O_{10}(OH)_2$) and quartz ($SiO_2$) [6].

2.1.1. Determination of Total Solids in Samples

In order to measure total solids a water sample was dried in hot air oven at 105 °C, by a porcelain dish. The sample volume was taken so that yield residue between 2.5–100 mg and was dried up to constant mass. Drying for 1 or 2 h was sufficient to reach constant mass, then the sample was cooled in a desiccator. The dish as soon as was cooled, was weighed to avoid absorption of moisture due to its hygroscopic nature. The mass of the dried residue was used to calculate the amount of solids in all samples Table 1.

2.1.2. Density Measurements

Density measurements were carried out with a graduated cylinder, carefully weighed and calibrated with distilled water. The density of distilled water, ρ_w, was measured with a portable densimeter (Mettler Portable 30PX). The cylinder filled with distilled water was weighed and its volume calculated by

$$V = \frac{m_w}{\rho_w}$$

The procedure was repeated by replacing the distilled water with the sample, then and the density for flocculated and non-flocculated samples is given by

$$\rho_{\text{sample}} = \frac{m_{\text{sample}}}{m_w}\rho_w$$

The results are summarized in Table 1.

Table 1. Solid content and density of the samples taken from the Occhito reservoir.

Flocculated Sample			Non Flocculated Samples		
% mass	Density kg m^{-3}	Cs kg m^{-3}	% mass	Density kg m^{-3}	Cs kg m^{-3}
12.9	1300	142	14.5	1365	162
1.2	1030	12.1	7.90	1200	83.7
6.8	1200	71.5	7.90	1200	83.7
4.4	1100	45.4	10.1	1254	109
6.1	1150	63.8	8.80	1221	93.9

2.2. Batch Settling Tests

A glass cylinder 5.0 cm in inside diameter and 25.4 cm high was used for containing the suspensions. It was graduated in 1-mm divisions and was kept vertical. The cylinder was illuminated with a lamp and sedimentation was monitored visually by measuring the height $H(t)$ of the moving front of

a nearly clear supernatant top layer against a lower layer suspension. The experimental apparatus is schematically illustrated in Figure 1.

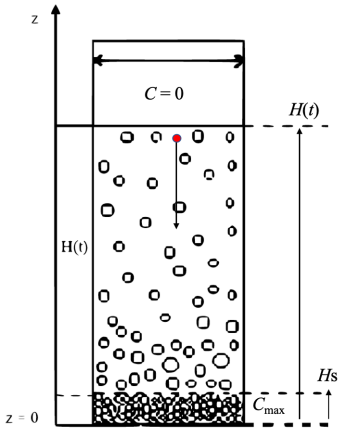

Figure 1. Schematic of the model used to describe sedimentation profiles.

2.3. Field Measurements

In order to reduce the water volume and increase concentration of solids, the dredged material is pumped in a geotexile tube. In other words, the geotube is a flexible and permeable container where suspended solids sediment generating a compact solid.

A simple diagram of the pumping system is shown in Figure 2, where the sampling points, P_1 and P_2, are indicated. The sample P_1 was intended to evaluate the effectiveness of the flocculant on the deposition rate of the solid material.

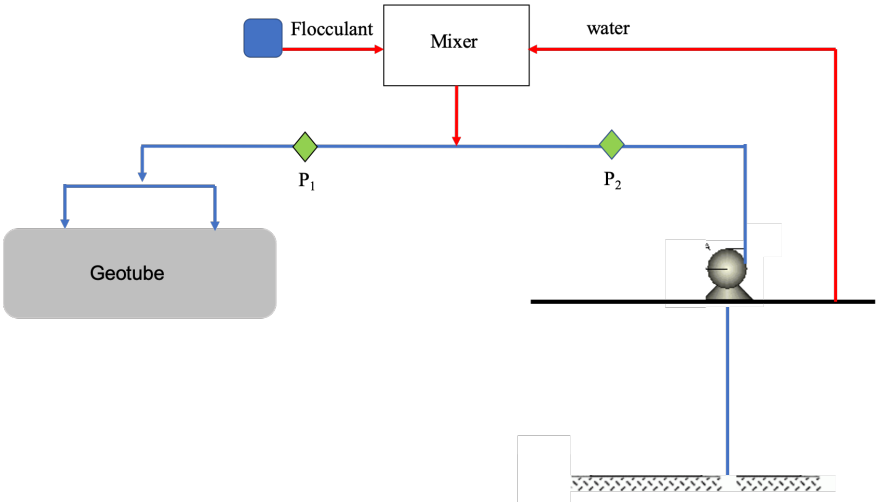

Figure 2. Schematic of the pumping plant used to empty Occhito reservoir. P_1 is the collection point of the material mixed with a polyacrylamide solution. P_2 is the pick-up point for material coming directly from the bottom of the reservoir.

2.4. Flocculant Dosage

In order to accelerate the sedimentation process and, therefore, to reduce the waiting times, in the stream of solids, a flocculant was introduced at a speed of $49.45 Lh^{-1}$. The flocculant was a cationic emulsion of polyacrylamide, Praestol K133 L, purchased from Solenis. The emulsion was pre-mixed with water from free surface of reservoir (see schematic of Figure 2).

2.5. Geotexile Tube Details

The geotexile structure is permeable fabric form (Geosyntex). It is filled with dredged soil from Occhito reservoir. A geotexile tube with high permeable fill material has better internal and external stability than non-permeablefabric form [12]. Geotubes used on the dredging site are made of polypropylene with a volume of $30 \times 7 \times 2.2$ m^3, $30 \times 9 \times 2.2$ m^3 and $30 \times 7 \times 2.5$ m^3.

3. Theoretical Background

Sedimentation Process

We consider the case of a particle falling vertically toward the bottom of a container in an incompressible viscous fluid, for instance the red particle in Figure 2. According to hydrodynamic laws, a particle of any size and shape moving with velocity u in a fluid of viscosity η is subjected to a drag force. If the difference between the force of resistance and the immersed weight of the particle (absolute weight minus the buoyancy force) is negative, the particle falls with an acceleration given by

$$\frac{du}{dt} = \left(1 - \frac{\rho}{\rho_s}\right)g - \frac{C_D u^2 \rho S}{2m} \tag{1}$$

where ρ_s, m and S are density, mass and surface of particle, respectively. C_D is the coefficient of drag and it is connected to dynamic properties of the system through the Reynolds number.

Although the coefficient C_D can be related to different motion regimes, Equation (1) refers to *free-fall* particles, therefore, it can only be used to analyze the hydrodynamic behavior of extremely diluted dispersions. In a real system when the gravitational force exceeds the buoyancy and drag forces, a concentration gradient builds up in the system with the larger particles moving faster to the bottom of the container. Hydrodynamic interactions between particles make the system very complex so that for the calculation of the fall speed it is convenient to develop semi-empirical approaches. That is to say a model which makes use of both laboratory results and fieldwork. In order to determine the settling rate, we choose an axis system with z-direction opposite to the velocity of particle motion. At time $t = 0$ the concentration of solids, C_0, is the same at any point. As time progress different zones are formed like, for instance, the supernatant at he top where $C = 0$ (*clear fluid*), and a zone of maximum concentration, C_{max}, at the bottom (see Figure 2). The concentration of suspended solids is a function of both position and time $C(z, t)$ and it determines the height of the interface between a particle-rich sediment and supernatant. Based on the principle of mass conservation, the interface height, $H(t)$, is defined as

$$\int_0^{H(t)} C(z,t)dz = H_0 C_0 \tag{2}$$

at any time $t > 0$.

Furthermore, in the region $z < H(t)$, the continuity equation provides

$$\frac{\partial C}{\partial t} - \frac{\partial (uC)}{\partial z} = 0 \tag{3}$$

Differentiation of Equation (2) with respect to time t yields

$$\int_0^{H(t)} \frac{\partial C}{\partial t} dz + \frac{dH}{dt} C(H(t), t) = 0 \tag{4}$$

Combination of Equation (4) with Equation (3) results

$$-\frac{dH}{dt} = u \tag{5}$$

Equation (5) relates the interface lowering to the accumulation speed of solids at the bottom of the container.

To illustrate the applicability of Equation (5) for settling process, let us make the assumption that at a given time $t = \theta$ the interface is to the position $z = H(\theta)$ and the average concentration of suspended solids is $C(\theta)$. The amount of material below the interface consists of particles made up of all the particles coarse enough to have settled the entire height H and particles of smaller size which not have settled. The total mass of solid is therefore

$$C_0 H_0 \mathcal{A} = C(\theta) H(\theta) \mathcal{A} + C(\theta) \mathcal{A} \theta \left(-\frac{dH}{dt} \right)_{t=\theta} \tag{6}$$

where $\mathcal{A}$ is the cross section of the cylinder. Solving Equation (6) with respect to $C(\theta)$, it is found.

$$C(\theta) = \frac{H_0 C_0}{H(\theta) + \theta \left(-\frac{dH}{dt} \right)_{t=\theta}} \tag{7}$$

This equation provides a rapid method for extracting the solid concentration at any time.

4. Results and Discussion

4.1. Sedimentation Profiles

The properties of dispersions are dependent on the particles size distribution, on the particle shape, and on the net interaction forces between the particles. In order to monitor such factors, sedimentation measurements are performed both on samples mixed with polyacrylamide and on samples polymer free. For each sample the height, $H(t)$, of the particle-rich phase as a function of time is measured. To compare the sedimentation profiles, the heights were first normalized to the initial height, as shown in Figure 3.

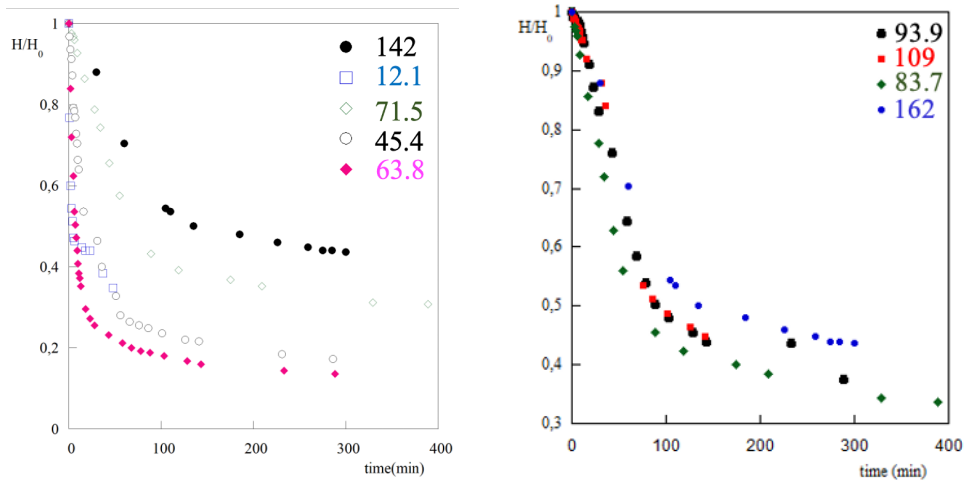

(**a**) (**b**)

Figure 3. Normalized sedimentation profiles. (**a**) Normalized sedimentation profiles of clay material polymer free. Dispersions from Occhito reservoir at different solids concentration (kg m^{-3}), indicated by numbers in the plot. (**b**) Normalized sedimentation profiles of dispersion mixed with polyacrylamide. Material from Occhito reservoir at different solids concentration, indicated by numbers in the plot.

Normalized sedimentation profiles of samples flocculant-free, for a large range of solids concentration, are shown in Figure 3a. As one can see these profiles are characterized by slow or non-existent settling for a finite waiting time. Furthermore, it is evident that the individual profiles are distinct from each other. The concentration range width is due to the dredger which

picks up the material at different depths. Figure 3b displays normalized sedimentation profiles of samples mixed with polyacrylamide, for different solids concentrations. Interestingly, these profiles can be scaled together onto a single curve. It is worth mentioning that organic polymeric flocculants, such as polyacrylamide, have a remarkable ability to aggregate even when added in small quantities. High molecular mass polymer with long chain is absorbed on solid particles attaching on *dangling* polymer segments onto other particles. Briefly, flocculation brought about by simultaneous co-adsorption of polymer molecules on two or more particles, i.e., *bridging flocculation*, generates denser clusters (*flocs*) with better settling characteristics [13]. In other words, a uniform particle-size distribution is generated, which gives a unique response to sedimentation. The high degree of "monodispersion" makes the system more easily manageable, therefore, the agglomerating function of the flocculant assumes a crucial role for optimizing of the dredging plant.

4.2. Master Curve

The evidence that all flocculated particles tend to distribute uniformly around an average size, suggests to normalize each sample to the final height, H_∞, of the solid-rich phase.

Therefore, we plot as a function of time, for each flocculated sample, the relative collapse of the particle-rich phase

$$Z(t) = \frac{H(t) - H_0}{H_\infty - H_0} \tag{8}$$

Interestingly, the curves can be all be scaled together onto a single muster curve. The shape of the curve does not vary for different solids concentration, the scaling behaviour remains robust even on a very large time scale. Indeed, Figure 4 shows the behavior of $Z(t)$ in an interval of 12,000 min. We can interpret this result as an effect of the flocculant which induces an attractive interaction between the particles creating a density mismatch between the particles and the suspending water. An analytical form of the function was obtained by means of a non-linear fitting procedure with two adjustable parameters, to all the experimental data.

$$Z(t) = 0.90 \frac{\frac{t}{64.1}}{1 + \frac{t}{64.1}} \tag{9}$$

where the value 64.1 min has to be considered a typical lifetime [14] of this material. Nonetheless the $Z(t)$ calculation is strongly dependent on the parameter H_∞, the height for completed settling process, i.e., at infinite time. This term depends on several factors so that it can be hardly deduced *a-priori*. First all, sedimentation measurements were carried out at very long times (3–4 days) in order to consider the settling process completely finished. The height of the interface measured under these conditions is H_∞ (red point in Figure 5). However, it is not practical to do so because the experimental procedure is time consuming. Furthermore, due to the compaction of the clayey material it is not always possible to carry out such measurements. A more useful alternate technique, therefore, is needed for calculation of H_∞ in dispersions. Such a technique is obtained by observing that H_∞ is defined by

$$\lim_{t \to \infty} H(t) = H_\infty \tag{10}$$

which can be rewritten as

$$\lim_{\frac{1}{t} \to 0} H\left(\frac{1}{t}\right) = H_\infty \tag{11}$$

In addition, it is experimentally verified that a plot $H(t)$ vs. $1/t$ exhibits a linear trend for a large range of variable t. Accordingly, H_∞ can readily be computed by a linear fit. The procedure is illustrated in Figure 5, where the value measured after four days is also shown for comparison. The maximum deviation between measured and extrapolated value is within 5%.

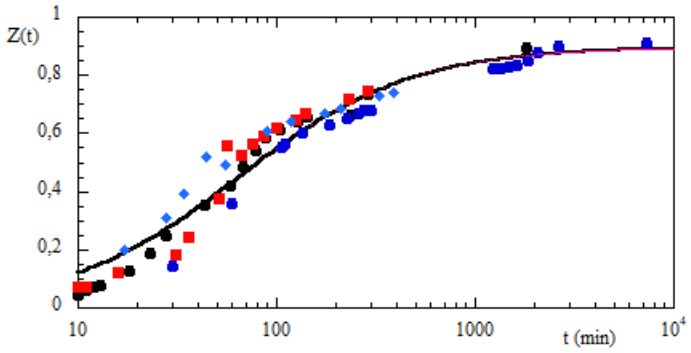

Figure 4. Master curve of clay material mixed with polyacrylamide. Samples from the Occhito reservoir.

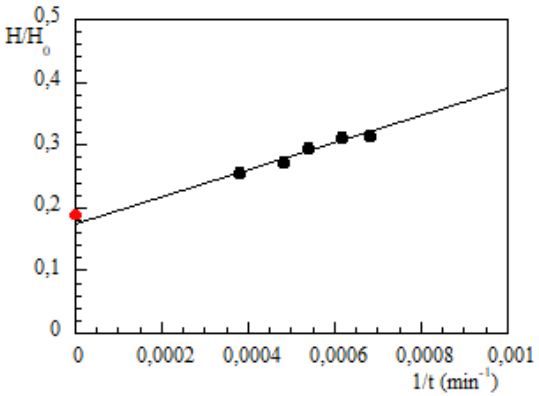

Figure 5. Procedure for extrapolating H_∞. The red dot represents the value of the normalized height measured after 4 days.

4.3. Sedimentation Rate

Sedimentation rate is an important quantity both to understand the phenomenon and to plan the drainage project. According to the definition of Equation (5) the function u can be deduced from sedimentation profiles provided that one knows how calculating the derivative of the function $H(t)$. Notwithstanding, experimental errors prevent a simple differential technique from being used to obtain the derivative. A method, already successfully used in the calculation of the partial molar volumes [15–17], the volume fraction distribution via self-diffusion measurements [18], the activation energy distribution function of complex reactions [19], and the degradation rate of indocyanine green in aqueous solution [20], is now proposed for computing, directly from experimental data, sedimentation rate.

In order to get a good estimate of the derivative at a point, a function must be fitted to several data points on both sides of that point. Then, the resulting function can be differentiated analytically. To do this, it is convenient to start at the top of the table of data and move step-wise down, evaluating the derivative at each center point by *arc moving* or *strip moving*. Furthermore, all experimental data require smoothing before differentiation is performed. Smoothing is performed herein by passing a least-squares polynomial through the data points to determine the polynomial coefficients and then replacing the experimental points with those calculated from the polynomial. The data points were smoothed, using five points in the movable strip and a third-degree polynomial. The smoothing was terminated at the stage where the random error was minimized. This technique is employed to calculate the sedimentation velocity and the solid concentration C_s by Equation (7).

Figure 6a displays a semilog plots of u vs. C_s for dispersions polymer free, interestingly these samples exhibit a linear trend, indicating an exponential decreasing. Figure 6b shows sedimentation rates of dispersions treated with a polyacrylamide solution. It is evident that even these dispersions exhibit a linear trend, however, the straight lines, within the experimental error, are parallel.

This means that the lifetime [14] of suspended particles is independent of solids concentration of solids accordingly particles exhibit a same falling speed. Once again, the effect is to be attributed to the polymer-induced bridging-flocculation.

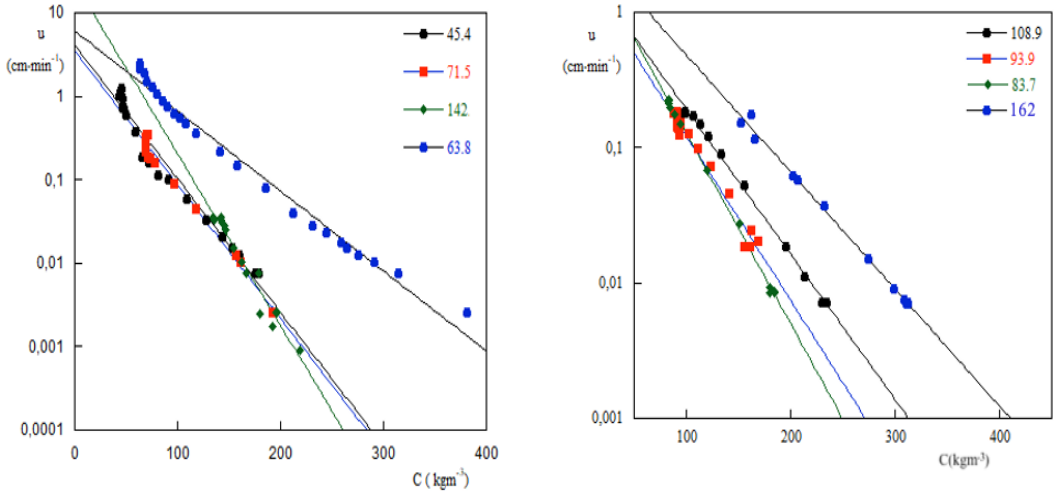

Figure 6. Sedimentation rates. (**a**) Normalized sedimentation profiles of clay material from Occhito reservoir. The numbers indicate concentrations (kg m^{-3}) of the solids. (**b**) Sedimentation rates computed for dispersion clays taken from Occhito's reservoir and not mixed with flocculant solution. The numbers represent the concentration (kg m^{-3}) of the solids.

4.4. Stage Semiempirical Model

To bring the water reservoir back to its original capacity, debris deposited on the bottom are dredged an pumped into a geotextile tube. The solids are retained inside the tube while the water flows out, therefore a certain number of passages are necessary to complete the drainage operation. Thus, overall process consists of a series of stages, each of which includes a filling step followed by the corresponding dewatering step. The total number of stages depends on the maximum capacity of the geotextile tube and on the cost of the entire purging operation. One of the essential requirements for a successful theory in technical models is judicious simplifications. The model presented here, starts from observation that that in the evacuation operations the dewatering time, t_D is always very long. Therefore, is reasonable to assume that at the end of each dewatering step solids in the geotube have attained the configuration they would have had in free settling process. This hypothesis allows to refine the model with experimental sedimentation results of material dredged by the reservoir.

Let us consider the j-th filling step, hence the solid material balance takes the form

$$Q_F^{(j)} t_F^{(j)} C_s^{F(j)} = V^{(j)}\left(t_F^{(j)}\right) C_s^{(j)}\left(t_F^{(j)}\right) \tag{12}$$

where $Q_F^{(j)}$ is the volume flow rate of clay material pumped to geotube, $t_F^{(j)}$ is the time taken for the j-th filling, $C_s^{F(j)}$ is the concentration of solids in the dredged material, $V^{(j)}\left(t_F^{(j)}\right)$ is the geotube volume after j-filling steps, at the time, $t_F^{(j)}$, $C_s^{(j)}\left(t_F^{(j)}\right)$ is the concentration of solids in the geotube at the time $\left(t_F^{(j)}\right)$. In each dewatering step the mass of the solids remains constant so that in j-th stage it must occur

$$\frac{d}{dt}\left\{V^{(j)}(t) C_s^{(j)}(t)\right\} = 0 \quad t_F^{(j)} \le t \le t_D^{(j)} \tag{13}$$

being $t_D^{(j)}$ the time to complete j-th dewatering step. Obviously, the volume of the geotube, $V^{(j)}(t)$, at j-th stage depends on the amount of water coming out.

Let $Q_w^{(j)}$ be volume flow rate of water, then we can write

$$V^{(j)}(t) = V^j\left(t_F^{(j)}\right) - \int_{t_F^{(j)}}^{t} Q(x)\mathrm{d}x \quad t_F^{(j)} \le t \le t_D^{(j)} \tag{14}$$

The function $Q_w^{(j)}$(t) contains into itself a term about which little is known except that it depends strongly on the fabric of which is made. Herein, we model volume water-flow by means of a two-parameter function

$$Q_w^{(j)}(t) = Q_w^{0(j)}\mathrm{erfc}\left(\frac{t - t_F^{(j)}}{\tau_j}\right) \tag{15}$$

where erfc(x) is the complementary error function, $Q_w^{0(j)}$ is the maximum water-flow rate and τ_j is the lifetime of j-th dewatering step.

Using this equation, Equation (14) can be easily integrated to yield

$$V^{(j)}(t) = V^{(j)}\left(t_F^{(j)}\right) - Q_w^{0(j)}\left[\left(t - t_F^{(j)}\right)\mathrm{erfc}\left(\frac{t - t_F^{(j)}}{\tau_j}\right) + \frac{1 - e^{\frac{\left(t - t_F^{(j)}\right)^2}{\tau_j^2}}}{\sqrt{\pi}}\tau_j\right] \tag{16}$$

Mass of solids remains constant for each dewatering step, therefore Equation (13) provides

$$C_s^{(j)}\left(t_D^{(j)}\right) = \frac{V^{(j)}\left(t_F^{(j)}\right)C_s^{(j)}\left(t_F^{(j)}\right)}{V^{(j)}\left(t_D^{(j)}\right)} \tag{17}$$

Equations (16) and (17) establish the concentration of solids and geotube volume after n stage, hence an economical evaluation of dredging project implemented can be carried out.

Let's consider the j-th dewatering step which starts with completely filled geotube, whose lateral surface is almost constant, then by using eq. we can write

$$Z\left(t_D^{(j)}\right) = \frac{H^{(j)}\left(t_D^{(j)}\right)}{H_{max}} \approx \frac{V^{(j)}\left(t_D^{(j)}\right)}{V_{max}} \tag{18}$$

Equation (16) provide a direct method to establish the geotube volume for each dewatering step and, then, concentration of solids collected after n stages. From what has been said about balance equations it is clear that the success of the method can be attained only by calculating parameters $Q_w^{0(j)}$ and τ_j of the model.

4.4.1. Calculation of Parameter $Q_w^{0(j)}$

To calculate this parameter we start from definition

$$Q_w^{0(j)} = \lim_{t \to 0}\left(-\frac{dV^{(j)}}{dt}\right) \tag{19}$$

In principle, such parameter can be directly measured on the dredging plant, however, an average value is predicatively more useful. Making use of Lagrange's Theorem [21], we write

$$\left(-\frac{dV^{(j)}}{dt}\right) = \frac{V^{(j)}\left(t_D^{(j)}\right) - V^{(j)}\left(t_F^{(j)}\right)}{t_D^{(j)} - t_F^{(j)}} \approx Q_w^{0(j)} \tag{20}$$

In reality, according to Lagrange's theorem the derivative in Equation (20) has to be calculated at a point inside the time interval $t_D^{(j)} \leq t \leq t_F^{(j)}$ [21], notwithstanding, if volume flow rate is slowly variable, Equation (20) gives an average value in the considered time-interval.

4.4.2. Calculation of Parameter τ_j

In order to compute this parameter we exploit the practical experience according to which $t_D^{(j)}$ is much longer than the corresponding $t_F^{(j)}$, hence we can write

$$V^{(j)}\left(t_D^{(j)}\right) = V_{max} - \int_0^{\infty} Q_w^{(j)}(t)\mathrm{d}t \tag{21}$$

Making use of Equations (16), (8), (20) and (21) we can write

$$\tau_j = \frac{\left(1 - Z\left(t_D^{(j)}\right)\right)V_{max}}{Q_w^{0(j)}}\sqrt{\pi} \tag{22}$$

These equations allow us to model the volume curves and solids concentration, for all dewatering steps. In order to design the entire purging process, one also has to model curves of filling steps. During filling steps the volume flow of stream entering the geotube is always kept constant, therefore the volume curve is a straight line whose equation is given by

$$V_F(t) = V\left(t_D^{(j-1)}\right) + \frac{V\left(t_F^{(j)}\right) - V(t_D^{(j-1)}}{t_F^{(j)} - t_D^{(j-1)}}\left(t - t_D^{(j-1)}\right) \quad t_D^{(j-1)} \leq t \leq t_F^{(j)} \tag{23}$$

with $t_D^{(0)} = 0$.

4.5. Numerical Application

The model developed in the previous sections is now used to analyze the $V(t)$ curve, i.e., the volume occupied by the solids in the geotextile tube as the process of removing clayey material from the Occhito reservoir progresses.

The length of times for each individual filling step were 56, 16 and 7 min, respectively, while durations of the corresponding dewatering steps were 1490, 178 and 1287 min. The maximum capacity of the geotextile tube was 330 m^3 and it was filled with a constant volume flow rate $Q_F = 7.2$ m^3 min^{-1} containing an initial concentration of solids $C_s^{0(F)} = 93.9$ kg m^{-3}. Numerical results are plotted in Figure 7, in the normalized form, together with some volume data collected directly on the dredging site. As one can see, the agreement is good and we are confident that by gathering more direct data, the model it will be able to be further refined.

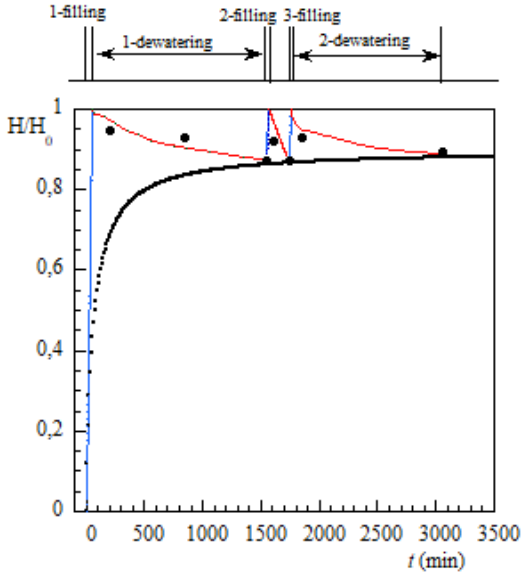

Figure 7. First three filling/dewatering stages of the process used to carry out the removal of Occhito reservoir. The dark dots are results of direct measurements on the geotextile tube.

5. Conclusions

One of the methods to restore the original capacity of a reservoir is to remove the material from bottom and collect it in geotexitile tubes. However, the clay is made up of very fine particle, which precipitate in long times making the process not economically sustainable. Therefore the settling process of solids in the geotubes is assisted by polymer, which act as flocculants. Laboratory measurements on these materials showed a uniform effect of the polymer on the particle-size so that sedimentation profiles of all samples follow the same master curve. This suggests scaling the experimental results to actual geotextile tube. A semi-empirical stage model is built from the idea that solids, at the end of each dewatering step, have reached the free sedimentation configuration. The model is then used to determine the first three filling/dewatering steps of the dredging process to restore the capacity of Occhito (Italy) reservoir. Curve $V(t)$ has been reconstructed, which indicates how the volume of solids in the geotube changes during the dredging operations. Model results are in good agreement with the data collected directly on site.

Author Contributions: Conceptualization, L.A.; B.M., Methodology, L.A.; B.M., numerical analyses were carried out by G.B.; A.D.V. reviewed, revised and improved the paper. All authors have read and agreed to the published version of the manuscript.

Funding: This research received no external funding.

Acknowledgments: The authors thank Ing. Giuseppe Di Nunzio of *Consorzio Bonifica Capitanata* for authorizing and helping to carry out surveys and measurements on the Occhito reservoir.

Conflicts of Interest: The authors declare no conflict of interest.

References

1. Covelli, C.; Cimorelli, L.; Pagliuca, D.N.; Molino, B.; Pianese, D. Assessment of Erosion in River Basins: A Distributed Model to Estimate the Sediment Production over Watersheds by a 3-Dimensional LS Factor in RUSLE Model. *Hydrology* **2020**, *7*, 13. [CrossRef]
2. De Vincenzo, A.; Molino, B.; Viparelli, R.; Caramuscio, P. A methodological approach for estimating turbidity in a river. *Int. J. Sediment Res.* **2011**, *26*, 112–119. [CrossRef]
3. Palermo, M. Disposal and placement of dredged material. In *Handbook of Dredging Engineering*, 5th ed.; McGraw-Hill: New York, NY, USA, 2000.

4. De Vincenzo, A.; Covelli, C.; Molino, A.J.; Pannone, M.; Ciccaglione, M.; Molino, B. Long-Term Management Policies of Reservoirs: Possible Re-Use of Dredged Sediments for Coastal Nourishment. *Water* **2019**, *11*, 15. [CrossRef]
5. De Vincenzo, A.; Molino, A.J.; Molino, B.; Scorpio, V. Reservoir rehabilitation: The new methodological approach of Economic Environmental Defence. *Int. J. Sediment Res.* **2017**, *32*, 288–294. [CrossRef]
6. Molino, B.; De Vincenzo, A.; Ferone, C.; Messina, F.; Colangelo, F.; Cioffi, R. Recycling of clay sediments for geopolymer binder production. A new perspective for reservoir management in the framework of Italian legislation: The Occhito reservoir case study. *Materials* **2014**, *7*, 5603–5616. [CrossRef] [PubMed]
7. Messina, F.; Ferone, C.; Molino, A.; Roviello, G.; Colangelo, F.; Molino, B.; Cioffi, R. Synergistic recycling of calcined clayey sediments and water potabilization sludge as geopolymer precursors: Upscaling from binders to precast paving cement-free bricks. *Constr. Build. Mater.* **2017**, *133*, 14–26. [CrossRef]
8. Hummer, C. DOER:"A major dredging research programme". *Terra et Aqua* **1998**, *72*, 13–17.
9. Fowler, J.; Bagby, R.M.; Trainer, E. Dewatering sewage sludge with geotextile tubes. In Proceedings of the 49th Canadian Geotechnical Conference, St. John's, NL, Canada, 23–25 September 1996; pp. 1–31.
10. Wortelboer, R. *Beneficial Use of Dredged Sediments Using Geotextile Tube Technology*; Digital Article; DredgDikes: Delft, The Netherlands, 2014.
11. Yee, T.; Lawson, C.; Wang, Z.; Ding, L.; Liu, Y. Geotextile tube dewatering of contaminated sediments, Tianjin Eco-City, China. *Geotext. Geomembr.* **2012**, *31*, 39–50. [CrossRef]
12. Leshchinsky, D.; Leshchinsky, O.; Ling, H.I.; Gilbert, P.A. Geosynthetic tubes for confining pressurized slurry: Some design aspects. *J. Geotech. Eng.* **1996**, *122*, 682–690. [CrossRef]
13. Lee, C.S.; Chong, M.F.; Robinson, J.; Binner, E. A review on development and application of plant-based bioflocculants and grafted bioflocculants. *Ind. Eng. Chem. Res.* **2014**, *53*, 18357–18369. [CrossRef]
14. Venditti, F.; Bufalo, G.; Lopez, F.; Ambrosone, L. Pollutants adsorption from aqueous solutions: The role of the mean lifetime. *Chem. Eng. Sci.* **2011**, *66*, 5922–5929. [CrossRef]
15. Ambrosone, L.; Costantino, L.; D'Errico, G.; Vitagliano, V. Density and viscosity studies of poly (ethylene-oxide) alkyl alcohols. *J. Solut. Chem.* **1996**, *25*, 757–772. [CrossRef]
16. Ambrosone, L.; Costantino, L.; D'errico, G.; Vitagliano, V. Thermodynamic and dynamic properties of micellar aggregates of nonionic surfactants with short hydrophobic tails. *J. Colloid Interface Sci.* **1997**, *190*, 286–293. [CrossRef] [PubMed]
17. Ambrosone, L.; Sartorio, R.; Vescio, A.; Vitagliano, V. Volumetric properties of aqueous solutions of ethylene glycol oligomers at 25 °C. *J. Chem. Soc. Faraday Trans.* **1996**, *92*, 1163–1166. [CrossRef]
18. Ambrosone, L.; Murgia, S.; Cinelli, G.; Monduzzi, M.; Ceglie, A. Size polydispersity determination in emulsion systems by free diffusion measurements via PFG-NMR. *J. Phys. Chem. B* **2004**, *108*, 18472–18478. [CrossRef]
19. Bufalo, G.; Ambrosone, L. Method for determining the activation energy distribution function of complex reactions by sieving and thermogravimetric measurements. *J. Phys. Chem. B* **2016**, *120*, 244–249. [CrossRef] [PubMed]
20. Di Nezza, F.; Guerra, G.; Costagliola, C.; Zeppa, L.; Ambrosone, L. Thermodynamic properties and photodegradation kinetics of indocyanine green in aqueous solution. *Dyes Pigments* **2016**, *134*, 342–347. [CrossRef]
21. Mateljević, M.; Svetlik, M.; Albijanić, M.; Savić, N. Generalizations of the Lagrange mean value theorem and applications. *Filomat* **2013**, *27*, 515–528. [CrossRef]